JOURNAL OF BONE AND MINERAL RESEARCH
Volume 24, Number 7, 2009
Published online on February 16, 2009; doi: 10.1359/JBMR.090204

Sustained BMP Signaling in Osteoblasts Stimulates Bone Formation by Promoting Angiogenesis and Osteoblast Differentiation

Fengjie Zhang,[1,2,3] Tao Qiu,[1] Xiangwei Wu,[1,3] Chao Wan,[1] Weibin Shi,[1] Ying Wang,[1] Jian-guo Chen,[2] Mei Wan,[1] Thomas L. Clemens,[1] and Xu Cao[1]

ABSTRACT: Angiogenesis and bone formation are tightly coupled during the formation of the skeleton. Bone morphogenetic protein (BMP) signaling is required for both bone development and angiogenesis. We recently identified endosome-associated FYVE-domain protein (endofin) as a Smad anchor for BMP receptor activation. Endofin contains a protein-phosphatase pp1c binding domain, which negatively modulates BMP signals through dephosphorylation of the BMP type I receptor. A single point mutation of endofin (F872A) disrupts interaction between the catalytic subunit pp1c and sensitizes BMP signaling in vitro. To study the functional impact of this mutation in vivo, we targeted expression of an endofin (F872A) transgene to osteoblasts. Mice expressing this mutant transgene had increased levels of phosphorylated Smad1 in osteoblasts and showed increased bone formation. Trabecular bone volume was significantly increased in the transgenic mice compared with the wildtype littermates with corresponding increases in trabecular bone thickness and number. Interestingly, the transgenic mice also had a pronounced increase in the density of the bone vasculature measured using contrast-enhanced μCT imaging of Microfil-perfused bones. The vessel surface and volume were both increased in association with elevated levels of vascular endothelial growth factor (VEGF) in osteoblasts. Endothelial sprouting from the endofin (F872A) mutant embryonic metatarsals cultured ex vivo was increased compared with controls and was abolished by an addition of a VEGF neutralizing antibody. In conclusion, osteoblast targeted expression of a mutant endofin protein lacking the pp1c binding activity results in sustained signaling of the BMP type I receptor, which increases bone formation and skeletal angiogenesis.
J Bone Miner Res 2009;24:1224–1233. Published online on February 16, 2009; doi: 10.1359/JBMR.090204

Keywords: bone morphogenetic protein, endofin, Smad1, bone formation, angiogenesis

Address correspondence to: *Xu Cao, PhD, 1670 University Boulevard, VH G003, Birmingham, AL 35294-0019, USA, E-mail: cao@uab.edu*

INTRODUCTION

In endochondral bone formation, bones are formed through the coupling of chondrogenesis with osteogenesis. During this process, blood vessel invasion from metaphysis coincides with mineralization of the extracellular matrix (ECM), apoptosis of hypertrophic chondrocytes, ECM degradation, and bone formation, suggesting crosstalk between angiogenesis and osteogenesis.[1–3] Angiogenesis is a multistep process that involves proliferation and migration of endothelial cells and generation of ECM.[4] It has been shown that many molecules are involved in the process including bone morphogenetic proteins (BMPs), vascular endothelial growth factor (VEGF), fibroblast growth factor (FGF), and TGFβ.[2,3]

BMPs, first identified as bone inductive growth factors in the TGFβ superfamily, are essential for skeletal development and known to induce both osteoblast and chondrocyte differentiation from mesenchymal cells.[5,6] Accumulated evidence has implicated BMPs in regulating the growth and development of many different tissues, in addition to cardiac and blood vessel.[7–9] BMPs stimulate vasculogenesis in the embryo and in adults, regulate endothelial–mesenchyme interactions during angiogenesis through Smad5, and activate endothelial growth through activation of VEGF/$VEGFR_2$ and angiopoietin/Tie2 signaling.[10–12] Moreover, during bone development and fracture healing, BMPs not only increase bone formation, but also enhance angiogenesis through regulating expression of VEGF.[13] VEGF, a prototypical angiogenic growth factor, plays important roles in regulation of proliferation, survival, and migration of endothelial cells.[14,15] Recent studies indicate that VEGF enhances BMP2-induced bone formation through modulation of angiogenesis.[16] Inhibition of VEGF blocks BMP2-induced angiogenesis and BMP4-induced bone formation.[3,17] These studies suggest that there is a close relationship and synergistic effect between BMPs and VEGF. However, it is currently unclear how BMPs might couple angiogenesis to bone formation.

The authors state that they have no conflicts of interest.

[1]Department of Pathology, University of Alabama at Birmingham, Birmingham, Alabama, USA; [2]Department of Pharmacology, Tongji Medical College, Huazhong University of Science and Technology, Wuhan, China; [3]Shihezi Medical College, Shihezi University, Xinjiang, China.

BMPs initiate their cellular action by binding to two receptors that have intrinsic serine/threonine kinase activity. Binding of ligand leads to the assembly of a hetero-oligomeric receptor complex, in which type II receptor phosphorylates and activates type I receptor. The activated type I receptor transiently associates with and phosphorylates Smad1. Once phosphorylated, Smad1 rapidly dissociates from the receptor and forms a complex with common-partner Smad, Smad4, and migrates into the nucleus, where the complex regulates the transcription of target genes.[18] Thus, the activity of this pathway is tightly controlled by serine/threonine phosphorylation, which transduces the cellular response from the plasma membrane into the nucleus.[19,20] Many studies show that protein phosphatase is directly involved in terminating the signal through dephosphorylation of these serine/threonine kinase or Smad1 in different signaling.[21–23] Previously, we showed that the endosome-associated FYVE-domain protein termed endofin acted as a Smad anchor for receptor activation in BMP signaling, which was similar to the function of SARA in TGFβ signaling. Endofin bound to Smad1 preferentially by the Smad-binding domain and enhanced Smad1 phosphorylation on BMP stimulation and also contained a protein–phosphatase binding domain, which recruited the catalytic subunit of protein phosphatase 1 (pp1c) and negatively modulated BMP signals through type I receptor dephosphorylation. Mutation of endofin pp1c binding domain enhanced BMP signaling and osteoblast differentiation in vitro.[24]

In this study, we created a mouse model with constitutive activation of BMP signaling specifically in osteoblasts using a mutant form of endofin with a defective pp1c binding domain. Expression of the endofin (F872A) mutant led to elevated levels of phosphorylated Smad1 in osteoblasts and augmented bone formation. Importantly, these mice also showed increased angiogenesis in vitro and in vivo. Our results indicate that recruitment of pp1c to endofin functions to negatively regulate the BMP signaling, and disruption of their interaction stimulates both angiogenesis and osteoblastic bone formation.

MATERIALS AND METHODS

Antibodies

The rabbit anti-endofin polyclonal antibody was raised against a peptide (amino acids 41–59, CSVSSELASSQR TSLLPKD) in the N terminus of human endofin with the assistance of Cytomol (Mountain View, CA, USA). Other antibodies were obtained from commercial sources: anti-actin mouse monoclonal antibody (Sigma-Aldrich), anti-phospho-Smad1 (Ser463/465) rabbit polyclonal antibody (Cell Signaling), anti-VEGF mouse monoclonal antibody (C-1; Santa Cruz), anti-osteocalcin rabbit polyclonal antibody (FL-95; Santa Cruz), and rat anti-mouse CD31 (PECAM-1) antibody (BD Biosciences Pharmingen).

Mice

The 2.3-kb mouse type I collagen (Col1α1-2.3) promoter was used to drive endofin (F872A) expression in generating the transgenic mice.[25] To generate the Col1α1-2.3 promoter-endofin (F872A) transgene, the lacZ reporter gene was removed by *Bam*H1 digestion from the pJ251 vector, which contains the Col1α1-2.3 promoter. Endofin (F872A) cDNA was cloned into the *Bam*H1 site of the pJ251 vector. The constructs were purified and microinjected into mouse (C57BL/6XSJL) eggs and surgically transferred to recipients by standard techniques. Tail tips were cut from pups at 2 wk of age and digested in homogenizing solution (10 mM Tris, pH 8.0, 100 mM NaCl, 20 mM EDTA, 1% SDS, and 0.5 mg/ml proteinase K) at 56°C for 12 h. Genomic DNA was extracted with phenol/chloroform. Genotyping was carried out by PCR. Specific primers designed for amplification of endofin (F872A) were 5′-CCAGGATGCCTGAAAG-3′ and 5′-GAAGTT CGCTGTGAGG-3′.

Skeletal phenotyping, histological analysis, and immunohistochemistry

X-ray analysis was performed in the intact right femurs obtained from both the mutant and wildtype (WT) mice at 16 wk of age using a Faxitron X-Ray machine (Faxitron, Wheeling, IL, USA). The bones were dissected free of soft tissues, fixed in 10% neutral buffered formalin for 48 h, and analyzed by a high-resolution μCT imaging system (MicroCT40; Scanco Medical). The scanner was set at a voltage of 55 kV and a current of 109 μA. Direct calculations of histomorphometric parameters were performed, including bone volume /total volume (BV/TV), trabecular thickness (Tb.Th), trabecular separation (Tb.Sp), and trabecular number (Tb.N).

Bone formation rates (BFRs) were measured by injection of two sequential doses of calcein (8 mg/10 ml sterile saline) delivered in a total of 0.25 ml 3 and 10 days before death. Bone histomorphometry analysis in undecalcified femoral sections was performed using the OsteoMeasure system (OsteoMetrics).

Immunohistochemistry was performed using standard protocols as recommended by the manufacturer (EnVision System; Dako). Briefly, mice femurs and tibias were dissected, fixed in 10% buffered formalin, decalcified in 10% EDTA, and embedded in paraffin. The bone sections were processed for antigen retrieval by digestion in 0.05% trypsin (pH 7.8) for 15 min at 37°C and incubated with antibodies against endofin (diluted 1:50), phospho-Smad1 (Ser463/465; diluted 1:50), VEGF (C-1; diluted 1:100), and osteocalcin (FL-95; diluted 1:100) overnight at 4°C. A horseradish peroxidase (HRP) streptavidin detection system (Dako) was subsequently used to detect the immunoactivity followed by counterstaining with hematoxylin (Sigma). Sections incubated with 1% nonimmune serum PBS solution served as negative controls. Quantitative immunostaining assay was performed by determining the percentage of positively stained cells in four random high-power fields (×400) that showed nuclear staining for P-Smad1 and cytoplasmic staining for osteocalcin. For osteocalcin staining assay, staining density was defined as weakly positive staining ($\leq +2$ in intensity) and strong positive staining ($\geq +3$ in intensity) on a scale

of 0 (no staining) to +4 (strongest intensity) in four adjacent sections.[26,27]

Imaging of blood vessels in bone

Blood vessels in bone were imaged by angiography of Microphil-perfused long bones.[28] The thoracic cavity was opened, and the inferior vena cava was severed after animals were killed. The vasculature was flushed with 0.9% normal saline containing heparin sodium (100 U/ml) at a pressure of ~100 mmHg through a needle inserted into the left ventricle. The specimens were pressure fixed with 10% neutral buffered formalin. Formalin was flushed from the vessels using heparinized saline, and the vasculature was injected with a radiopaque silicone rubber compound containing lead chromate (Microfil MV-122; Flow Tech). Samples were stored at 4°C overnight for contrast agent polymerization. Mouse femurs were dissected from the specimens and soaked for 4 days in 10% neutral buffered formalin to ensure complete tissue fixation. Specimens were subsequently treated for 48 h in a formic acid–based solution (Cal-Ex II) to decalcify the bone and facilitate image thresholding of the femoral vasculature from the surrounding tissues. Images were obtained using a high-resolution (16-μm isotropic voxel size) μCT imaging system. A threshold of 306 was initially chosen based on visual interpretation of thresholded 2D tomograms. Histomorphometric parameters including vessel volume, vessel surface, and vessel volume per tissue volume (VV/TV) were evaluated.

Fetal mouse metatarsal angiogenesis assay

Metatarsal explant cultures were performed as described previously.[29] Briefly, E17.5 embryos were removed from timed-pregnant mice, and metatarsals were dissected. The isolated metatarsals were cultured in 24-well tissue culture plates in 150 μl of αMEM supplemented with 10% heat-inactivated FBS and 1% of penicillin/ streptomycin for 72 h. Two hundred fifty microliters of fresh medium was replaced, and metatarsals were cultured for 14 days, with replacement of medium every 3 days. Explants were fixed in zinc formalin for 15 min at room temperature and subsequently stained for CD31 using a rat polyclonal antiserum against mouse CD31 (diluted 1:50). Cultures were performed in sextuplicate, and each complete experiment was repeated at least twice.

Primary osteoblast culture and bone marrow stromal cell culture

Primary osteoblasts were isolated from calvariae of newborn mice by serial digestion in 1.8 mg/ml of collagenase type I (Worthington Biochemical) solution. Calvariae were digested in 10 ml of digestion solution for 15 min at 37°C under constant agitation. The digestion solution was collected repeatedly for total of five times. Digestion solutions 3–5, which contained the osteoblasts, were pooled together. After centrifugation, osteoblasts were obtained and cultured in αMEM containing 10% FBS and 1% penicillin/streptomycin at 37°C in a humidified incubator supplied with 5% CO_2.

For bone marrow stromal cell culture, mice were killed at 10–14 days of age, and the femurs and tibias were dissected free of soft tissues under sterile conditions. The bone marrow cells were collected after rinsing with syringe and plated onto a 100-mm petri dish. On the second day, medium was removed, and the cultures were gently rinsed with PBS twice and cultured in αMEM medium containing 10% FBS, 1% penicillin/streptomycin, and 1% glutamine. Medium was changed every 3 days until the cells became confluent.

Alkaline phosphatase and von Kossa staining

Primary cells were plated on 6-well plates with a density of 2×10^5 cells/well and cultured in αMEM until they were confluent. Medium was changed to osteogenic medium with the addition of β-glycerophosphate (10 mM) and ascorbic acid (50 μg/ml) to αMEM. Cells were cultured for 14 days, with the medium changed every 3 days. Histochemical staining for alkaline phosphatase (ALP) activity in the cells was determined using Sigma Fast BCIP/NBT Tablets (B5655) according to the manuals. von Kossa staining was carried out by adding 3% silver nitrate solution to formalin-fixed cells and exposing cells to UV light. The deposits of calcium were shown by the formation of opaque mineralized nodules. Densitometric analysis of ALP was performed using NIH ImageJ 1.38b.

Western blot analysis

Total protein extracted from freshly dissected whole bone of the mutant mice for endofin (F872A) protein expression or whole cell lysate was obtained by cell lysis buffer in the presence of a protease inhibitor cocktail. Forty micrograms of protein extracts was loaded onto an SDS mini-PAGE system after concentrations were determined by the Bradford method. After electrophoresis, proteins were transferred to a PVDF membrane using a Bio-Rad semi-dry transfer system. Protein transfer efficiency and size determination were verified using prestained protein markers. Membranes were blocked with 5% dry milk in Tris-buffered saline Tween-20 for 1 h at room temperature and subsequently incubated overnight with primary antibodies at 4°C. Signals were detected using an HRP-conjugated secondary antibody and the Super-Signal West Femto Maximum Sensitivity Substrate (Thermo Scientific). Antibodies were used as described above.

RT-PCR

Total RNA was extracted from primary osteoblasts using the RNA STAT-60 method as recommended by the manufacturer (Tel-Test). The yield and purity of RNA was estimated spectrophotometrically using the A260/A280 ratio. Five micrograms of RNA was reverse transcribed into cDNA using the SuperScript first-strand synthesis system (Invitrogen). One microliter of cDNA was subjected to PCR amplification using SYBR GREEN PCR Master Mix (Promega) and sequence-specific primers for VEGF: 5′-CCACGTCAGAGAGCAACATCA-3′

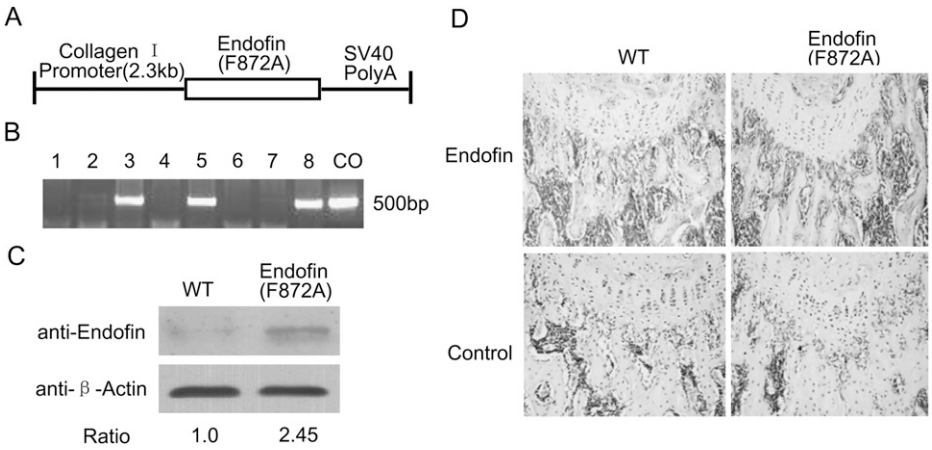

FIG. 1. Generation of transgenic mice with point mutation in endofin (F872A). (A) Diagram of expression construct of endofin (F872A) driven by 2.3-kb mouse type I collagen promoter (Col1α1) for generation of transgenic mice. (B) Representative genotyping of endofin (F872A) transgenic mice by PCR analysis of expression of endofin (F872A). Lanes 3, 5, and 8 represent the mutant transgene, whereas lanes 1, 2, 4, 6, and 7 represent WT littermates. CO, positive control. (C) Western blot analysis of protein extracted from bone tissue of WT littermates and the mutant for endofin (F872A) expression. The ratio of mutant endofin to endogenous endofin was 2.45. (D) Representative histological sections of distal femurs from WT and endofin (F872A) transgenic mice with immunostaining with an antibody against endofin.

and 5′-TCATTCTCTCTATGTGCTGGCTTT-3′. PCR reactions were performed in triplicate, and endogenous mouse GAPDH was used as internal control.

Statistical analysis

All data are presented as mean ± SD. Student's *t*-test was used for comparison of histomorphometric parameters. For quantitative analysis of immunostaining data, Student's *t*-test was performed followed by a χ^2 test. A significance level was defined as $p < 0.05$.

RESULTS

Characterization of mice with overexpression of an endofin mutant (F872A) protein

We showed that introduction of a point mutation of endofin at the pp1c-binding domain (F872A) results in enhanced BMP signaling and accelerates osteoblast differentiation *in* vitro.[24] To examine the role of endofin in osteoblasts in vivo, we generated transgenic mice expressing an endofin cDNA encoding the point mutation (F872A) driven by a 2.3-kb type I collagen promoter (Fig. 1A). Three transgenic lines were established (Fig. 1B), two of which were evaluated in more details for their bone phenotype. Expression of the endofin (F872A) transgene was confirmed by immunoblotting of extracts of whole bone from 1-mo-old transgenic mice, and the expression level of endofin (F872A) in the transgene mice was nearly 2.5-fold that of the endogenous endofin level in WT mice (Fig. 1C). Immunostaining of femoral sections from the transgenic mice clearly showed enhanced expression of endofin in osteoblasts lining the trabecular bone of the proximal metaphyseal region (Fig. 1D).

Bone formation and osteoblast surface are increased in endofin (F872A) transgenic mice

We next examined the effect of endofin (F872A) on bone acquisition in mice. X-ray analysis of long bones showed an increase in bone mass of the transgenic mice compared with WT littermates at 16 wk of age (Fig. 2A). μCT measurement on femurs from 16-wk-old transgenic mice showed an increase in bone volume particularly in trabecular bone (Fig. 2B). Transgenic mice had significantly increased trabecular bone volume, number, and thickness and decreased trabecular bone separation compared with their WT littermates (Figs. 2C–2F). To further examine the impact of the mutant endofin on the increased bone formation, both the static and dynamic bone histomorphometric analyses were quantified. Transgenic mice showed increased bone formation rate (Figs. 2G and H) and mineralizing surface (Fig. 2I) accompanied by increased osteoblast surface (Fig. 2J), whereas osteoclast surface was slightly increased compared with WT littermates (Fig. 2K). Collectively, these data suggest that sustained BMP signaling in the osteoblast from mice expressing the mutant endofin (F872A) for pp1c binding activity contributes to the increased bone accumulation by increasing both surface and activity of resident osteoblasts.

Osteoblast differentiation is enhanced in endofin (F872A) mutant mice

To determine the mechanism responsible for the increased bone formation, we cultured primary cells from endofin transgenic mice and their WT littermates. Western blot analysis showed that the level of endogenous phosphorylated Smad1 (P-Smad1) was elevated in endofin transgenic mice in comparison with that in WT littermates (Fig. 3A), indicating that mutation of pp1c binding

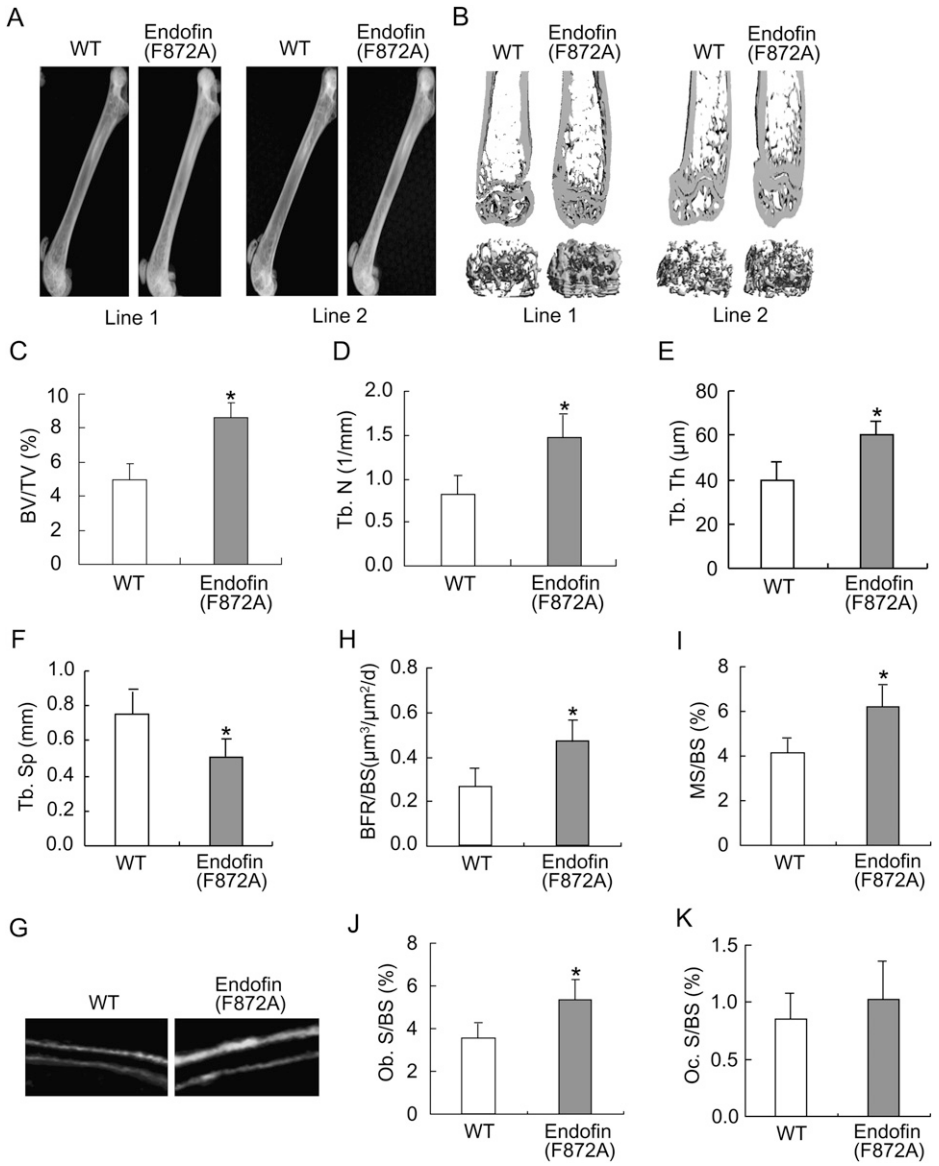

FIG. 2. Increased bone formation in endofin (F872A) mutant mice. (A and B) Increased BMD is shown (A) in radiography and (B) μCT images of femur of endofin (F872A) mutant mice and their WT littermates at 16 wk of age. Two lines were shown. Quantitation of bone structure by μCT shows comparison of endofin mutant mice (gray bars) with their WT littermates (white bars), increased (C) bone volume per tissue volume (BV/TV), (D) trabecular number (Tb.N), (E) trabecular thickness (Tb.Th.), and decreased (F) trabecular separation (Tb.Sp). (G) Dynamic parameter bone formation rate (BFR) was assessed by two sequential doses of calcein injection in mice at 6 wk of age before death. Representative calcein-labeled sections of proximal tibias are visualized by fluorescence micrography. Bone histomorphometric analysis of trabecular bone of the femur, (H) bone surface referent bone formation rate (BFR/BS), (I) mineralizing surface per bone surface (MS/BS), and (J) osteoblast surface per bone surface (Ob.S/BS) were increased in endofin (F872A) mutant mice, but there is no significant difference in osteoclast surface per bone surface (Oc.S/BS) between endofin (F872A) mutant mice and their WT littermates (K). Quantitative data are expressed as means ± SD. $*p < 0.05$, $n = 4$.

domain of endofin enhanced BMP signaling. Moreover, the degree of differentiation as determined in cells exposed to ascorbate and β-glycerol phosphate–containing medium was enhanced as assessed by staining for ALP and mineral deposition (von Kossa). ALP activity and bone mineralization were enhanced in the endofin mutant transgenic mice (Figs. 3B–3E). In addition, osteocalcin expression by determined by Western blot analysis was also increased in the osteoblasts from the transgenic mice (Fig. 3F).

To determine whether BMP signaling was enhanced in mice expressing the endofin mutation in vivo, we compared the levels of P-Smad1 in sections of bone from mutant and WT mice. Immunostaining of the femoral sections with an antibody specific for P-Smad1 confirmed that the mice expressing the mutant endofin had increased levels of P-Smad1 (Figs. 3G and 3H) in osteoblasts. Immunostaining showed increased levels of osteocalcin indicating that osteoblast differentiation was stimulated in the mutant mice (Figs. 3I–3J). These results suggest that enhanced BMP signaling derived from endofin mutation promotes osteogenesis.

Angiogenesis is enhanced in skeleton of endofin (F872A) mutant mice

At necropsy, we noted that the long bones from the endofin mutants were more richly perfused with blood compared with control bones (Fig. 4A), suggesting that angiogenesis during bone development was enhanced in the mutants. To examine the impact of the endofin mutation on bone vasculature, we performed contrast-enhanced μCT imaging in Microfil-perfused bones. These studies showed a significant increase in the density of the vasculature in the endofin (F872A) mutant mice at 2 mo of age (Fig. 4B). Morphometric analysis showed that vessel

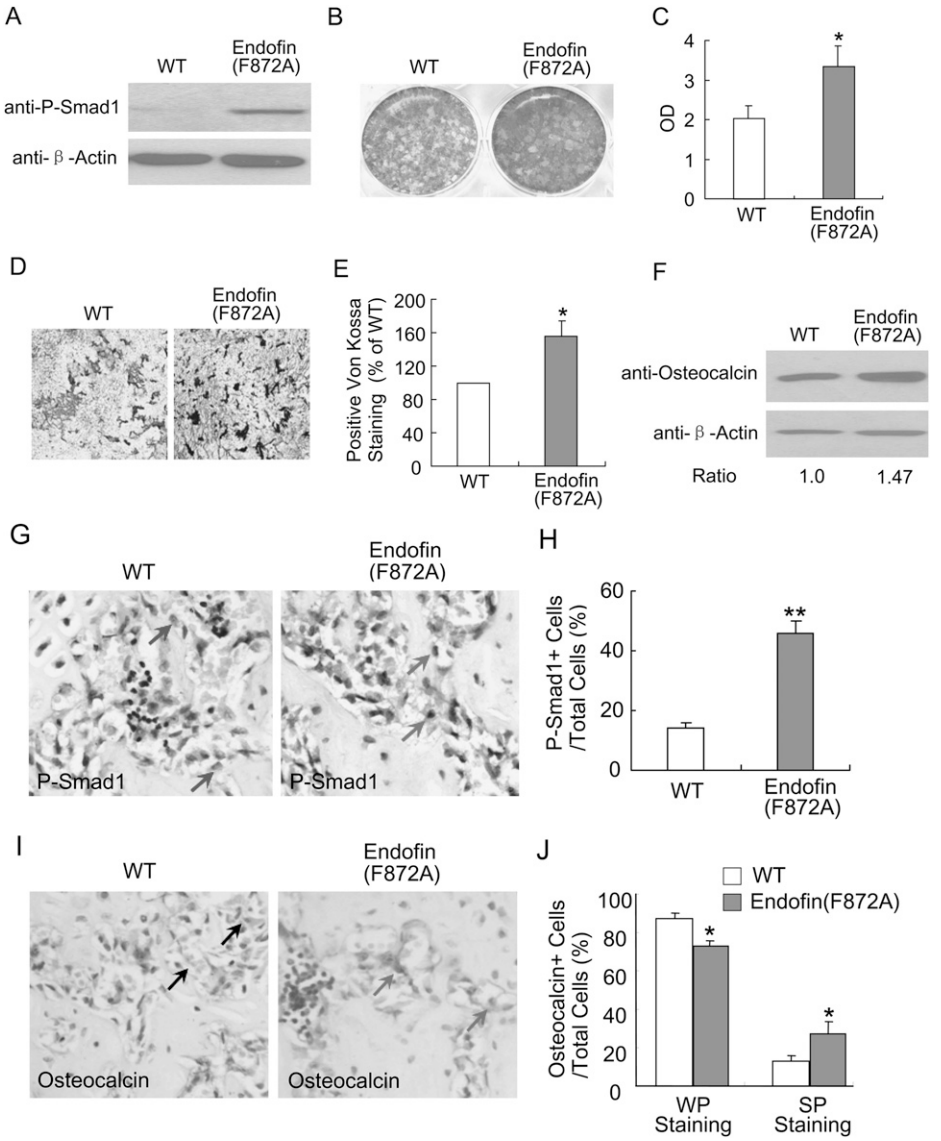

FIG. 3. Enhanced osteoblastic differentiation in endofin (F872A) mutant mice. Primary pre-osteoblasts isolated from either endofin (F872A) mutant mice or their WT littermates were cultured in osteogenic medium. (A) Western blot analysis shows that endogenous phosphorylated Smad1 (P-Smad1) levels of the primary calvaria osteoblast were increased in endofin (F872A) mutant mice relative to the WT mice. Endogenous β-actin was used as internal control. (B) Representative micrographs of histochemical staining of ALP in calvarial pre-osteoblasts isolated from endofin (F872A) mutant mice or their WT littermates. Before staining, the primary pre-osteoblasts were cultured in osteogenic medium for 14 days. (C) Quantitative densitometric analysis of ALP activity in B using NIH Image J 1.38. (D) Representative micrographs of von Kossa staining for mineralized nodule formation in pre-osteoblasts cultured in osteogenic medium for 21 days. (E) Quantification of von Kossa–stained mineralized nodules is expressed as percent of WT pre-osteoblast staining. Ten randomly selected microscopic fields were examined in each of three independent experiments. Quantitative data represent mean ± SD. $*p < 0.05$. (F) Western blot analysis shows that endogenous osteocalcin expression of the primary pre-osteoblasts was increased in endofin (F872A) mutant mice relative to the WT mice. The ratio of osteocalcin expressed in the mutant mice to the control mice was 1.47. Endogenous β-actin was used as internal control. (G) Immunostaining of femoral sections for P-Smad1 and (H) quantitative analysis of the nuclear expression of P-Smad1 shows that the level of P-Smad1 was increased in endofin (F872A) mutant mice relative to that of WT mice. Sections were counterstained with hematoxylin. Gray arrows indicate positive staining. Total cells represent the cells covering the bone surface. Quantitative data represent mean ± SD. $**p < 0.01$. (I) Immunostaining of femoral sections for osteocalcin and (J) quantitative analysis of the expression of osteocalcin in density shows that the level of osteocalcin was higher in endofin (F872A) mutant mice than WT mice. Black arrows indicate weakly positive staining (WP staining). Gray arrows indicate strong positive staining (SP staining). Total cells represent the cells covering the bone surface. Quantitative data represent mean ± SD. $*p < 0.05$.

surface and volume were both increased in endofin mutant mice relative to controls (Figs. 4C and 4D). The ratio of vessel volume and total volume was also increased (Fig. 4E). Angiogenesis assays using explants of E17.5 mouse metatarsals showed greater endothelial sprouting in rudiments from the mutant mice compared with controls (Fig. 4F). These results indicate that sustained BMP receptor signaling in osteoblasts of the mice expressing

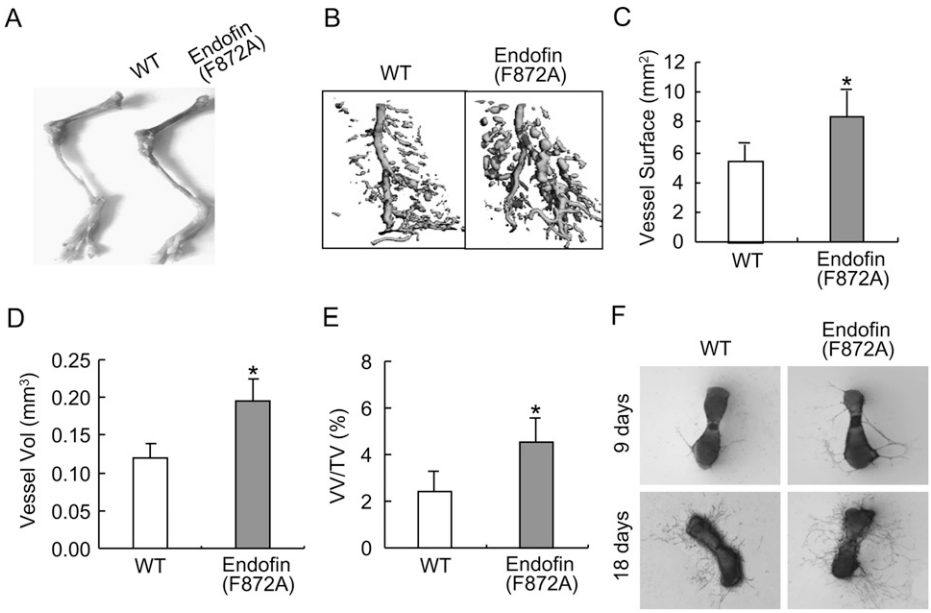

FIG. 4. Stimulated angiogenesis in long bones of endofin (F872A) mutant mice. (A) Photograph of hind limbs from endofin (F872A) mutant mice and their WT littermates. (B) Representative μCT images of vasculature in Microfil-perfused femurs from 2-mo-old endofin (F872A) mutant mice and their WT littermates. Quantitative μCT angiography analysis shows increased vessel surface (C), vessel volume (D), and ratio of vessel volume/total volume (VV/TV) (E) within femoral bone of endofin (F872A) mutant mice (gray bars) relative to control mice (white bars). Data represent mean ± SD. $*p < 0.05$. $n = 5$. (F) Representative images show increased endothelial sprouting in metatarsals from endofin (F872A) mutant mice in an in vitro angiogenesis assay at 9 and 18 days, respectively. The metatarsals were dissected from E17.5 fetuses of endofin (F872A) mutant mice and their WT littermates. Endothelial sprouting is visualized by immunostaining for CD31. Magnification, ×25.

the endofin mutation increase both angiogenesis and osteogenesis.

Angiogenesis is induced through osteoblast-derived VEGF

VEGF is a recognized angiogenic factor in bone and cartilage,[3,30] and BMPs are known to stimulate expression of VEGF in bone marrow stromal cells and osteoblasts.[13,31] Therefore, the expression of VEGF in primary osteoblastic cells was examined with both RT-PCR and Western blot. The levels of both VEGF mRNA and protein were significantly increased in the cells from endofin mutant mice compared with those of their WT littermates (Figs. 5A and 5B). Immunostaining of the femoral sections with antibody specific against VEGF showed that the VEGF protein level was also increased relative to control mice (Fig. 5C).

To determine the requirement for VEGF for the increased angiogenesis seen in the endofin mutant mice, an angiogenesis assay was performed using explants of E17.5 mouse metatarsals. Basal endothelial sprouting was enhanced in metatarsals of endofin mutant mice relative to that of their WT littermates (Fig. 5D). Importantly, addition of a VEGF neutralizing antibody almost entirely blocked the endothelial sprouting. Taken together, these results indicate that elevated VEGF expression from sustained BMP signaling in osteoblasts stimulates angiogenesis during bone formation.

DISCUSSION

In this study, we provide in vivo evidence that sustained BMP signaling in osteoblasts increases bone formation by driving osteoblast differentiation and stimulating angiogenesis in developing bone. By targeting a mutant form of endofin with defective binding to pp1c, a negative regulator of BMP signaling, we created a mouse model for osteoblast-specific, constitutive activation of BMP signaling in osteoblasts. These mice developed greater bone mass accompanied with increased vascularity, suggesting that BMP controls osteoblast performance through both cell autonomous and cell nonautonomous mechanisms. Most importantly, the mouse model provides novel insights on the interaction between BMP signaling and blood vessel development in bone.

Because BMPs and their receptors are widely expressed and exert many functions, it has been difficult to assign specific actions of these growth factors.[32–34] This is particularly a problem in skeletal tissue, which is composed of a number of cell types with each one playing a role in balancing bone formation with bone resorption. The identification of the inhibitory domain in endofin provided the means to activate BMP signaling specifically and constitutively in specific cells types. Signaling through receptors of the TGFβ superfamily is mediated by cytoplasmic Smad proteins.[18] SARA for Smad anchor for receptor activation facilitates TGFβ and activin/nodal signaling by

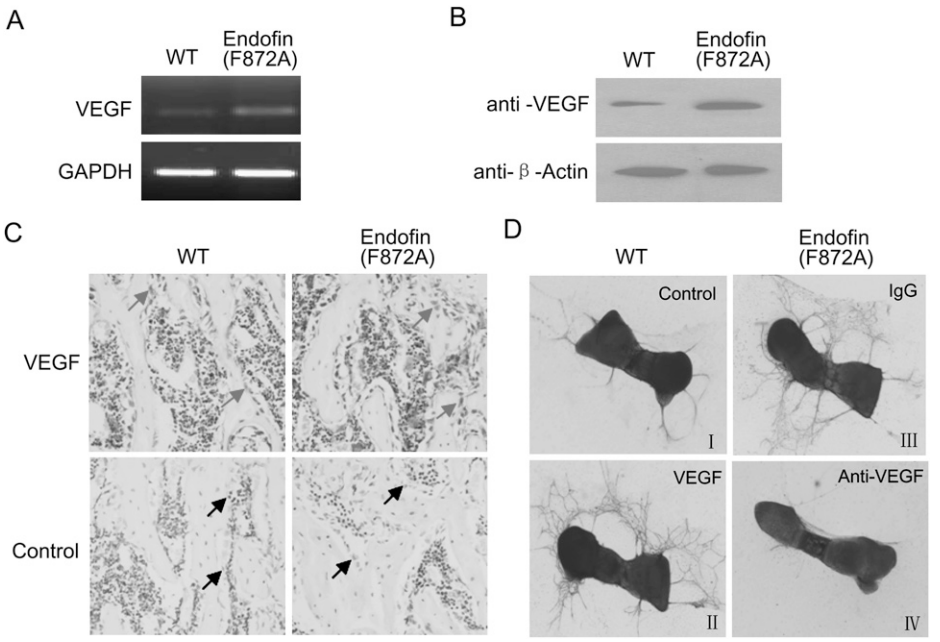

FIG. 5. Increased expression of VEGF necessary for the enhanced angiogenesis in endofin (F872A) mutant mice. (A) Levels of VEGF mRNA in primary osteoblasts measured by RT-PCR. The primary cells were isolated from endofin (F872A) mutant mice or their WT littermates and cultured under osteogenic medium for 18 days before harvesting of total RNA. (B) Western blot analysis shows increased expression of VEGF protein in osteoblasts as prepared in A. (C) Immunostaining of femoral sections with the anti-VEGF antibody shows increased VEGF expression (gray arrows) in endofin (F872A) mutant mice relative to control mice. Nonimmune serum was used as negative control. Black arrows indicate negative staining in osteoblast. Magnification, ×400. (D) Representative images show endothelial sprouting in metatarsals from endofin (F872A) mutant mice and WT littermates, which were treated with the different serums described below. (I) Metatarsal from WT littermates. (II) Metatarsal from WT littermates treated with recombinant VEGF (10 ng/ml). (III) Metatarsal from endofin (F872A) mutant mice treated with mouse IgG (100 ng/ml). (IV) Metatarsal from endofin (F872A) mutant mice treated with a VEGF-neutralizing antibody (100 ng/ml). Data are representative of three independent experiments.

recruiting and presenting Smad2/3 to the receptor complex.[35] Like SARA, endofin contains a protein-phosphatase–binding motif, which negatively modulate BMP signals through dephosphorylation of BMPRI, whereas overexpression of WT endofin does not enhance BMP signaling in vitro and in vivo.[24] Thus, targeted overexpression of this mutant protein in osteoblasts leads to sustained BMP signaling only in osteoblasts. Under these conditions, constitutive activation of BMP signaling produced expected increases in bone formation likely by enhancing the ability of bone marrow stromal cell (MSC) precursors to differentiate into mature osteoblasts.

These studies suggest that VEGF production is stimulated in the osteoblast on BMP activation and is required for angiogenesis during bone development. VEGF has emerged as a pleiotropic mediator of angiogenesis and hematopoiesis, and its importance during bone formation has been shown by a number of previous studies.[28,29,36] Major sites of VEGF production are the osteoblast and the growth plate, where it is regulated by the hypoxia inducible factors (HIFs).[29,37] Mice overexpressing HIFs in osteoblasts had increased VEGF with greatly increased angiogenesis and bone formation and bone regeneration.[38] Thus, it seems that VEGF might serve to link angiogenesis to osteogenesis during development. The studies presented in this paper show that BMP signaling in osteoblasts also increases VEGF, suggesting that BMP signaling may be part of an autocrine loop necessary for the linkage of bone formation and angiogenesis. In agreement with this idea, treatment of MSCs with GDF-5 promoted osteogenic differentiation of rat fat–derived stromal cells in association with increased angiogenic and VEGF gene expression in vitro.[31]

These results also indicate that sustained BMP signaling in the osteoblast of the endofin mutant expressing mice occurred as the result of both direct effects on the osteoblast (cell autonomous) and indirect (cell non autonomous) effects. Thus, enhanced BMP signaling in the endofin mutant mice increased MSC differentiation when assessed in vitro. Elevated VEGF expression derived from sustained BMP signaling promotes angiogenesis and the following osteogenesis. In contrast, neutralizing antibodies against VEGF entirely blocked endothelial sprouting from the endofin (F872A) expressing metatarsals (Fig. 5D). These effects are unlikely caused by VEGF itself, because this angiogenic molecule has little effect on osteoblast performance at least measure by proliferation and differentiation in vitro, despite the presence of both VEGF receptors.[30] These results suggest an in vivo model in which VEGF and other angiogenic mediators are produced in close proximity in the stroma. We predict that VEGF acts on the endothelium to elicit an as yet unidentified molecule that acts in a paracrine model to directly stimulate bone progenitor cell differentiation. Further testing of this idea

will require new experimental models with which to manipulate both VEGF and BMP signaling in the bone microenvironment. Such studies should more precisely define the mechanism for coupling angiogenesis and osteogenesis during bone development and could also lead to more effective therapeutic approaches to augment bone mass and speed bone repair after injury.

ACKNOWLEDGMENTS

The authors thank the UAB Center for Metabolic Bone Disease Cores for mouse animal genotyping and histomorphometric analyses. This work was supported by National Institutes of Health Grant DK57501 to X.C. and AR049410 to T.C.

REFERENCES

1. Adams SL, Cohen AJ, Lassová L 2007 Integration of signaling pathways regulating chondrocyte differentiation during endochondral bone formation. J Cell Physiol **213:**635–641.
2. Gerber HP, Ferrara N 2000 Angiogenesis and bone growth. Trends Cardiovasc Med **10:**223–228.
3. Carano RA, Filvaroff EH 2003 Angiogenesis and bone repair. Drug Discov Today **8:**980–989.
4. Coultas L, Chawengsaksophak K, Rossant J 2005 Endothelial cells and VEGF in vascular development. Nature **438:**937–945.
5. Chen D, Ji X, Harris MA, Feng JQ, Karsenty G, Celeste AJ, Rosen V, Mundy GR, Harris SE 1998 Differential roles for bone morphogenetic protein (BMP) receptor type IB and IA in differentiation and specification of mesenchymal precursor cells to osteoblast and adipocyte lineages. J Cell Biol **142:**295–305.
6. Ryoo HM, Lee MH, Kim YJ 2006 Critical molecular switches involved in BMP-2-induced osteogenic differentiation of mesenchymal cells. Gene **366:**51–57.
7. Carev D, Saraga M, Saraga-Babic M 2008 Involvement of FGF and BMP family proteins and VEGF in early human kidney development. Histol Histopathol **23:**853–862.
8. van Wijk B, Moorman AF, van den Hoff MJ 2007 Role of bone morphogenetic proteins in cardiac differentiation. Cardiovasc Res **74:**244–255.
9. Langenfeld EM, Langenfeld J 2004 Bone morphogenetic protein-2 stimulates angiogenesis in developing tumors. Mol Cancer Res **2:**141–149.
10. Moser M, Patterson C 2005 Bone morphogenetic proteins and vascular differentiation: BMPing up vasculogenesis. Thromb Haemost **94:**713–718.
11. Yang X, Castilla LH, Xu XL, Li CL, Gotay J, Weinstein M, Liu PP, Deng CX 1999 Angiogenesis defects and mesenchymal apoptosis in mice lacking SMAD5. Development **126:** 1571–1580.
12. Suzuki Y, Montagne K, Nishiara A, Watabe T, Miyazono K 2008 BMPs promote proliferation and migration of endothelial cells via stimulation of VEGF-A/VEGFR2 and angiopoietin-1/Tie2 signalling. J Biochem **143:**199–206.
13. Deckers MM, van Bezooijen RL, van der Horst G, Hoogendam J, van Der Bent C, Papapoulos SE, Löwik CW 2002 Bone morphogenetic proteins stimulate angiogenesis through osteoblast-derived vascular endothelial growth factor A. Endocrinology **143:**1545–1553.
14. Ferrara N, Gerber HP, LeCouter J 2003 The biology of VEGF and its receptor. Nat Med **9:**669–676.
15. Hicklin DJ, Ellis LM 2005 Role of the vascular endothelial growth factor pathway in tumor growth and angiogenesis. J Clin Oncol **23:**1011–1027.
16. Samee M, Kasugai S, Kondo H, Ohya K, Shimokawa H, Kuroda S 2008 Bone morphogenetic protein-2 (BMP-2) and vascular endothelial growth factor (VEGF) transfection to human periosteal cells enhances osteoblast differentiation and bone formation. J Pharmacol Sci **108:**18–31.
17. Peng H, Wright V, Usas A, Gearhart B, Shen HC, Cummins J, Huard J 2002 Synergistic enhancement of bone formation and healing by stem cell-expressed VEGF and bone morphogenetic protein-4. J Clin Invest **110:**751–759.
18. Heldin CH, Miyazono K, Tendijke P 1997 TGF-beta signalling from cell membrane to nucleus through SMAD proteins. Nature **390:**465–471.
19. Derynck R, Zhang YE 2003 Smad-dependent and Smad-independent pathways in TGF-beta family signalling. Nature **425:**577–584.
20. Attisano L, Wrana JL 2002 Signal transduction by the TGF-beta superfamily. Science **43:**635–639.
21. Knockaert M, Sapkota G, Alarcon C, Massague J, Brivanlou AH 2006 Unique players in the BMP pathway: Small C-terminal domain phosphatases dephosphorylate Smad1 to attenuate BMP signaling. Proc Natl Acad Sci USA **103:**11940–11945.
22. Shi WB, Sun CX, He B, Xiong WC, Shi XM, Yao DC, Cao X 2004 GADD34-PP1c recruited by Smad7 dephosphorylates TGFβ type I receptor. J Cell Biol **164:**291–300.
23. Bennett D, Alphey L 2002 PP1 binds Sara and negatively regulates Dpp signaling in *Drosophila melanogaster*. Nat Genet **31:**419–423.
24. Shi WB, Chang CB, Nie SY, Xie ST, Wan M, Cao X 2007 Endofin acts as a Smad anchor for receptor activation in BMP signaling. J Cell Sci **120:**1216–1224.
25. Zhao M, Harris SE, Horn D, Geng ZP, Nishimura R, Mundy GR, Chen D 2002 Bone morphogenetic protein receptor signaling is necessary for normal murine postnatal bone formation. J Cell Biol **157:**1049–1060.
26. Grizzle WE, Myers RB, Manne U, Stockard CR, Harkins LE, Srivastava S 1998 Factors affecting immunohistochemical evaluation of biomarker expression in Neoplasia. In: Margaret H, Zbigniew W (eds.) John Walker's Methods in Molecular Medicine—Tumor Marker Protocols. Humana Press, Totoma, NJ, USA, pp. 161–179.
27. Qiu T, Grizzle WE, Oelschlager DK, Shen X, Cao X 2007 Control of prostate cell growth:BMP antagonizes androgen mitogenic activity with incorporation of MAPK signals in Smad1. EMBO J **26:**346–357.
28. Wan C, Gilbert SR, Wang Y, Cao X, Shen X, Ramaswamy G, Jacobsen KA, Alaql ZS, Eberhardt AW, Gerstenfeld LC, Einhorn TA, Deng L, Clemens TL 2008 Activation of the hypoxia-inducible factor-1alpha pathway accelerates bone regeneration. Proc Natl Acad Sci USA **105:**686–691.
29. Wang Y, Wan C, Deng LF, Liu XM, Cao XM, Gilbert SR, Bouxsein ML, Faugere MC, Guldberg RE, Gerstenfeld LC, Haase VH, Johnson RS, Schipani E, Clemens TL 2007 The hypoxia-inducible factor a pathway couples angiogenesis to osteogenesis during skeletal development. J Clin Invest **117:**1616–1626.
30. Gerber HP, Vu TH, Ryon AM, Kowalski J, Werb Z, Ferrara N 1999 VEGF couples hypertrophic cartilage remodeling, ossification and angiogenesis during endochondral bone formation. Nat Med **5:**623–628.
31. Sena K, Sumner DR, Virdi AS 2007 Modulation of VEGF expression in rat bone marrow stromal cells by GDF-5. Connect Tissue Res **48:**324–331.
32. Dewulf N, Verschueren K, Lonnoy O, Moren A, Grimsby S, Vandespiegle K, Miyazono K, Huylebroeck D, Tendijke P 1995 Distinct spatial and temporal expression patterns of 2 type-I receptors for bone morphogenetic proteins during mouse embryogenesis. Endocrinology **136:**2652–2663.
33. Enomoto-Iwamoto M, Iwamoto M, Mukudai Y, Kawakami Y, Nohno T, Higuchi Y, Takemoto S, Ohuchi H, Noji S, Kurisu K 1998 Bone morphogenetic protein signaling is required for maintenance of differentiated phenotype, control of proliferation, and hypertrophy in chondrocytes. J Cell Biol **140:**409–418.
34. Liu D, Wang J, Kinzel B, Mueller M, Mao XH, Valdez R, Liu YX, Li E 2007 Dosage-dependent requirement of BMP type II

receptor for maintenance of vascular integrity. Blood **110:** 1502–1510.
35. Tsukazaki T, Chiang TA, Davison AF, Attisano L, Wrana JL 1998 SARA, a FYVE domain protein that recruits Smad2 to the TGF beta receptor. Cell **95:**779–791.
36. Bluteau G, Julien M, Magne D, Mallein-Genin F, Weiss P, Daculsi G, Guicheux J 2007 VEGF and VEGF receptors are differentially expressed in chondrocytes. Bone **40:**568–576.
37. Schipani E, Didrickson S, Kobayashi T, Knight M, Johnson RS 2001 Hypoxia in cartilage: Hif-1alpha is essential for chondrocyte growth arrest and survival. Genes Dev **15:**2865–2876.
38. Towler DA 2007 Vascular biology and bone formation: hints from HIF. J Clin Invest **117:**1477–1480.

Received in original form August 5, 2008; revised form November 24, 2008; accepted February 11, 2009.